Available online at www.sciencedirect.com
ScienceDirect
Mendeleev Commun., 2024, **34**, 587–590

Mendeleev Communications

Hydrogenation of dinitrobenzenes over titania-supported palladium nanoparticles

Elena V. Shuvalova* and Olga A. Kirichenko

N. D. Zelinsky Institute of Organic Chemistry, Russian Academy of Sciences, 119991 Moscow, Russian Federation. Fax: +7 499 135 5328; e-mail: evshouvalova@yandex.ru

DOI: 10.1016/j.mencom.2024.06.039

Catalysts of 1% Pd/TiO_2 type were prepared *via* the deposition–precipitation of Pd polyhydroxo complexes followed by reduction with hydrogen at 23 °C. These catalysts were found to be active for the selective hydrogenation of *m*-dinitrobenzene into *m*-phenylenediamine at 25–50 °C and 0.5 MPa H_2 in a batch reactor.

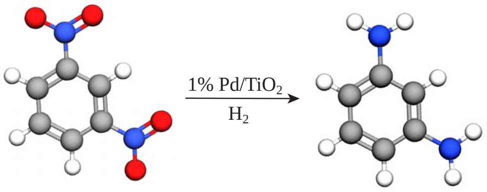

Keywords: hydrogenation, dinitrobenzene, phenylenediamine, Pd/TiO_2 catalysts, hydrogen.

Conventional reduction of aromatic nitro compounds (ANCs) with disulfides or metal–acid systems to produce the corresponding amines is still of practical importance,[1,2] while the catalytic ANC reduction with molecular hydrogen is preferable.[3–6] The catalytic hydrogenation can be performed in a solvent-free mode or in a solution (in an organic solvent or in water) at an elevated hydrogen pressure using the catalysts based on nanoparticles (NPs) of Pd, Pt, Ru, Rh, Au, Ni and Cu supported on different carbons and other supports.[3,7–16] The catalyst selectivity and stability can be improved by using reducible TiO_2 and CeO_2 supports *via* enhancing the metal–support interaction and optimizing adsorption of the nitro group.[3,17–19] Comparison of TOF values for the supported palladium catalysts in the solvent-free nitrobenzene hydrogenation revealed the following sequence of the used commercial oxide supports: $CeO_2 \gg SiO_2 > ZrO_2 \gg \gg Al_2O_3 > La_2O_3$.

The oxide- and carbon-supported Pd NPs were highly active and selective catalysts[6–8,19–24] for partial hydrogenation of halo nitrobenzene, nitrostyrene, nitrophenol, nitrobenzaldehyde, nitroacetophenone, and other mono-, di- and trinitroarenes. The 2.5% Pd/CeO_2 catalyst almost completely transformed 32 functional ANCs with high selectivity to the corresponding aromatic amines in the absence of a solvent under the following conditions: p_{H_2} = 2.0 MPa, the molar ratio substrate/Pd = 2820, the reaction temperature 40–210 °C (5–45 °C higher than the substrate melting point) and the reaction time varied within 0.5–20 h depending on the substrate nature.[19] Complete conversion of 4-nitrophenol with almost 100% selectivity to aminophenol was reached over the 3% Pd/Fe_3O_4 catalyst in 52 min at 60 °C, 0.1 MPa H_2 and the molar ratio substrate/Pd = 177.[7] Palladium NPs deposited on the carbon supports (Sibunit, carbon blacks) *via* hydrolytic deposition of Pd polynuclear hydroxy complexes (PHCs) (1–4% Pd) were effective in selective hydrogenation of ethyl 4-nitrobenzoate[20] even at 30–50 °C and 0.1 MPa H_2 and allowed one to achieve a complete conversion of the substrate with a benzocaine yield about 100% in 1 h under mild reaction conditions: 50 °C, 0.5 MPa H_2, and the molar ratio substrate/Pd = 540.[8,21] The similar catalysts 1% Pd/CNG (Pd supported on nanocarbon globules) were also highly active in the liquid-phase hydrogenation of ANCs to the corresponding valuable amines, and they provided 99.9% selectivity to aromatic amines at almost complete conversion under mild conditions (50 °C, 0.5 MPa, 1 h).[8] The successful hydrogenation of trinitrobenzene and its derivatives with a high yield of amines was performed over the Pd/Sibunit catalysts prepared by the PHC technique, the Pd loading of 1 wt% being preferable as to 5 wt% due to the shorter reaction time and the higher yield of the target products.[22–24]

Surprisingly, hydrogenation of dinitrobenzene (DNB), *e.g.*, *m*-DNB **1** (Scheme 1) over Pd catalysts was poorly studied,[25–27] although *m*-phenylenediamine (*m*-PDA) **3** is a valuable chemical of growing demand. Hydrogenation of *m*-dinitrobenzene (*m*-DNB) **1** over the 5% Pd/C catalyst resulted in the 90% conversion at 31 °C and 3.4 MPa H_2, yet the major product was *m*-nitroaniline (*m*-NA) **2** with a selectivity of 95%.[28] The 2.5% Pd/CeO_2 catalyst also provided complete hydrogenation of *m*-DNB **1** only to *m*-NA **2** in a solvent-free mode at 95 °C, 2.0 MPa and the high molar ratio DNB/Pd = 2800.[19] Recent application of the three-dimensional hydrophobic polymers including Pd nanoclusters for the hydrogenation of *m*-DNB **1** in water exhibited complete transformation to *m*-PDA **3** in 8 h at 25 °C, 0.1 MPa H_2 and the molar ratio DNB/Pd = 760.[29] Based on this fact and keeping in mind that NA **2** can be reduced to PDA **3** over Pd catalysts in 60–80 min under mild conditions,[7,8] it makes sense to look for reasonable mild conditions of **1** → **3** hydrogenation over supported Pd NPs.

The present work was aimed to reveal the catalytic behavior of Pd NPs supported on the commercial TiO_2 (P-25) carriers in

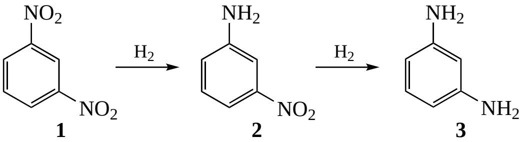

Scheme 1

the direct hydrogenation of *m*-DNB **1** with molecular hydrogen. The catalysts were prepared by the deposition–precipitation method *via* hydrolytic deposition of Pd PHCs on the TiO_2 surface followed by reduction to Pd^0 with H_2 at 23 °C in a slurry[30] (the catalyst preparation procedure is described in Online Supplementary Materials). Two as-prepared catalysts with the same Pd loading of 1 wt% differed in the size (d) and dispersion (γ) of supported metallic Pd NPs, which were calculated based on CO chemisorption[30] and equal to 5.0 nm and 23% for Pd/T1 and to 6.9 nm and 16% for the Pd/T2 catalyst. The catalysts were tested in hydrogenation of *m*-DNB **1** in accordance with the protocol given in Online Supplementary Materials. Both catalysts provided a high *m*-DNB **1** conversion in 15 min even at room temperature, yet selectivity to amines was low (Figures 1 and 2), which can be due to the major contribution of stable intermediates such as aromatic nitroso, hydroxyamino and azoxy/azo/hydrazo compounds.[26,31] The selectivity to *m*-NA **2** was relatively high in the beginning of the reaction especially at the minimal molar ratio n_{DNB}/n_{Pd} = 240, but decreased at a higher substrate/catalyst loading of 590 [see Figure 1(*b*)]. The further hydrogenation of intermediates and *m*-NA **2** resulted in the formation of *m*-PDA **3** with a selectivity higher than 90% in 1–2.5 h depending on an initial *m*-DNB **1** concentration in the reaction mixture, a molar ratio n_{DNB}/n_{Pd} and a catalyst sample (Figures 1 and 2, Table 1). At a larger initial *m*-DNB **1** concentration (C_{0DNB}) of 0.15 M, the selectivity to *m*-PDA **3** reached the values higher than 90% already in 60 min, while in the 0.06 M solution 150 min were required to achieve such a high selectivity to *m*-PDA **3** (see Figure 1) despite more than twice lower loading n_{DNB}/n_{Pd} = 240. These facts indicate a stronger dependence of reaction rates on C_{0DNB} for both *m*-NA **2** and *m*-PDA **3** formations than the rates for appearance of intermediates. It was pointed out previously[26,32] that all hydrogenation steps in the process were first order to reactants. Elevation of the reaction temperature to 50 °C accelerated the *m*-PDA **3** formation. An almost fivefold increase in TOF was observed at the lowest C_{0DNB} and loading for the Pd/T1 sample (Table 2), and a selectivity higher than 90% was reached already in 15 min (see Figure 2). For the Pd/T2 sample, the effect was weaker, probably due to the larger Pd NPs size. At larger loadings, a double increase in TOF was observed (see Table 2). The time of complete DNB **1** conversion at the same C_{0DNB} significantly increased with loading, and the time and value of the highest selectivity to DNB varied as well (Figure 3). At the highest loading of 780, the relatively high selectivity to intermediate *m*-NA **2** was revealed as a curve with a maximum in a wide interval of the reaction time.

The found variations in the conversion and selectivity may be explained by the complicated mechanism and parameters of the

Table 1 Hydrogenation of *m*-DNB over 1% Pd/TiO_2 catalysts.[a]

Catalyst	n_{DNB}/n_{Pd}	$C_{0\,DNB}$/ mol dm^{-3}	*T*/°C	*t*/min	Selectivity to *m*-PDA (%)
Pd/T1	240	0.06	25	120	96.3
	240	0.06	50	15	98.6
	590	0.15	25	60	95.6
	590	0.15	50	30	95.0
	780	0.06	50	150	90.8
	780	0.12	50	75	98.3
Pd/T2	240	0.06	25	90	95.6
	240	0.06	50	15	90.7

[a] Teflon-lined 100 ml autoclave, ethanol (20 ml), catalyst loading 0.05 g, and 0.5 MPa H_2; *m*-DNB conversion >99.9%.

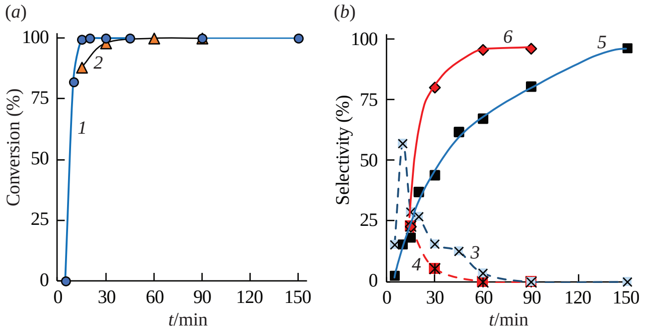

Figure 1 Time dependences of (*a*) *m*-DNB **1** conversion and (*b*) selectivity to NA **2** and PDA **3** over the Pd/T1 sample (d_{Pd} = 5.0 nm) (C_{0DNB} = 0.06 M or 0.15 M; *T* = 25 °C; p_{H_2} = 0.5 MPa). Curves *1, 3, 5* relate to n_{DNB}/n_{Pd} = 240, and curves *2, 4, 6* relate to n_{DNB}/n_{Pd} = 590; curves *3, 4* relate to selectivity for NA **2**, and curves *5, 6* relate to selectivity for PDA **3**.

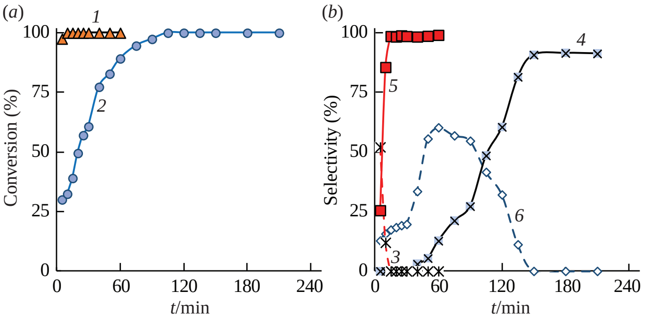

Figure 3 Time dependences of (*a*) *m*-DNB conversion and (*b*) selectivity to NA **2** and PDA **3** over the Pd/T1 sample (C_{0DNB} = 0.06, *T* = 50 °C; p_{H_2} = 0.5 MPa). Curves *1, 3, 5* relate to n_{DNB}/n_{Pd} = 240, and curves *2, 4, 6* relate to n_{DNB}/n_{Pd} = 780; curves *3, 6* relate to selectivity for NA **2**, and curves *4, 5* relate to selectivity for PDA **3**.

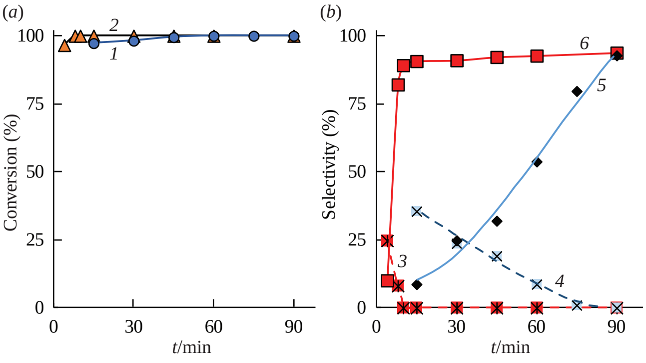

Figure 2 Time dependences of (*a*) *m*-DNB **1** conversion and (*b*) selectivity to NA **2** and PDA **3** over the Pd/T2 sample (d_{Pd} = 6.9 nm), (C_{0DNB} = 0.06 M; $n_{DNB}:n_{Pd}$ = 240; p_{H_2} = 0.5 MPa). Curves *1, 4, 5* relate to *T* = 25 °C, and curves *2, 3, 6* relate to *T* = 50 °C; curves *3, 4* relate to selectivity for NA **2**, and curves *5, 6* relate to selectivity for PDA **3**.

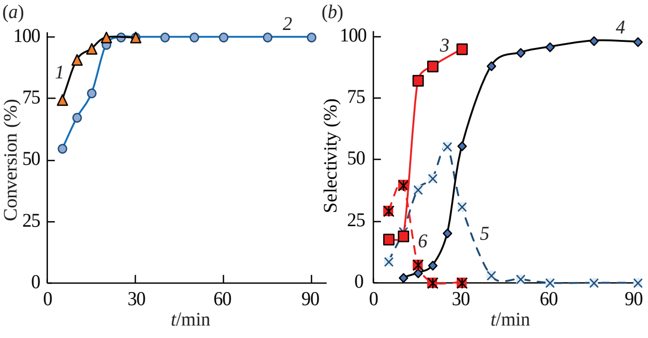

Figure 4 Time dependences of (*a*) *m*-DNB conversion and (*b*) selectivity to NA **2** and PDA **3** over the Pd/T1 sample, (C_{0DNB} = 0.12 and 0.15 M, *T* = 50 °C; p_{H_2} = 0.5 MPa). Curves *1, 3, 6* relate to n_{DNB}/n_{Pd} = 590, and curves *2, 4, 5* relate to n_{DNB}/n_{Pd} = 780; curves *5, 6* relate to selectivity for NA **2**, and curves *3, 4* relate to selectivity for PDA **3**.

Table 2 Catalytic activity of Pd catalysts in hydrogenation of *m*-DNB.[a]

Catalyst[b]	Molar ratio DNB/Pd	$C_{0\mathrm{DNB}}$/mol dm^{-3}	T/°C	TOF/s^{-1}	STY/h^{-1}	Reference
Pd/T1	240	0.06	25	0.21	120	this work
	240	0.06	50	1.07	950	this work
	590	0.15	25	0.57	570	this work
	590	0.15	50	1.13	1120	this work
	780	0.06	50	0.38	280	this work
	780	0.12	50	0.80	610	this work
Pd/T2	240	0.06	25	0.22	150	this work
	240	0.06	50	0.60	870	this work
0.7 Pd@3D-HPOPs-1	760	0.1	25	–	95	29
Pt/CeO_2-ZrO_2	117[c]	0.1	25	–	39	18
n Ni_3Pt/SiO_2	140[c]	0.1	25	–	70	25
Pd/T1	860[d]	0.08[d]	50	6.6	1700	this work
1Pd/CNG	860[d]	0.08[d]	50	–	860	8

[a] TOF is the number of PDA molecules formed per one surface Pd atom per second. It was calculated in the beginning of the reaction at a PDA yield below 25%. The STY is the total amount of PDA (mol) produced per Pd amount unit (mol) per hour. It was calculated at the highest selectivity to the product and the complete substrate conversion. [b] Dispersity and the average Pd NP size are 23% and 5.0 nm for Pd/T1, as well as 16% and 6.9 nm for Pd/T2. [c] Hydrogenation of *m*-DNB over Pt catalysts. [d] Hydrogenation of nitrobenzene.

corresponding kinetic model. Although the reaction mechanism and the kinetic model were developed only for *m*-DNB **1** hydrogenation over the commercial 5% Pt/C and 20% Ni/SiO_2 catalysts,[26] it is likely that for a Pd catalyst they are similar. According to the proposed mechanism,[26] *m*-DNB **1** was first reduced to *m*-NA **2**, and then consecutive hydrogenation to *m*-nitrosoaniline, *m*-(hydroxyamino)aniline and *m*-PDA occurred simultaneously with condensation of *m*-(hydroxyamino)-aniline and *m*-nitrosoaniline followed by hydrogenolysis of the thus formed azoxy compound to *m*-PDA **3**. The concentration curves of the kinetic model developed for the proposed mechanism have shown that the *m*-NA **2** mole concentration first increased and then decreased. This may indicate the formation of the intermediate azoxy compound (not registered by GC) whose concentration can be relatively high in the course of the process and would finally decrease due to its slow hydrogenolysis. The mole concentration of *m*-PDA **3** increased with the reaction time.

The total productivity of the catalysts under different conditions was estimated using the site time yield (STY) that was calculated as a total amount of PDA (moles) produced per Pd amount unit (moles) per hour. The obtained STY values were large even at room temperature and exceeded the best values published[25] for Pd and Pt catalysts (see Table 2). Since there are no data for *m*-DNB **1** hydrogenation over Pd/C catalysts prepared using hydrolytic deposition of Pd PHCs, for comparison, we performed hydrogenation of nitrobenzene under the conditions similar to those previously reported.[8] The results of these experiments exhibited that the catalyst on the TiO_2 support was more active, and at 50 °C and 0.5 MPa H_2, the complete conversion with selectivity to *m*-DNB **3** of 98.2% was reached in 0.5 h, which resulted in about a double STY (see Table 2).

In contrast to successful fast selective hydrogenation of *m*-DNB **1** to *m*-PDA **1**, hydrogenation of *p*-DNB over Pd/T1 proceeded considerably slower. Only a 83% *p*-DNB **1** conversion with 8.7% selectivity to *p*-NA **2** was observed at 50 °C in 2 h, and no *p*-PDA was observed within 8 h at 50 °C. Nevertheless, at a higher (70 °C) temperature, a complete *p*-DNB conversion was reached in 4 h, the selectivity to *p*-NA **2** of 57% was achieved in 6 h, and *p*-PDA appeared in 8 h reaching 47% selectivity in 18 h. A considerable decrease in the catalytic activity may be due to the use of THF as a solvent instead of ethanol because of very low *p*-DNB **2** solubility in ethanol, as it was shown previously[8] that the use of THF instead of aqueous ethanol decreased the hydrogenation activity (TOF) of supported Pd NPs in ANC reduction more than an order of magnitude.

Summarizing, complete conversion of *m*-DNB **1** with 91–99% selectivity to *m*-PDA **1** and the high STY of 120–1120 h^{-1}, which considerably exceeded the best previously reported results over different catalysts, has been reached in a batch mode hydrogenation at the high molar loading $n_{\mathrm{DNB}}/n_{\mathrm{Pd}}$ = 240–780 under mild conditions (25–50 C, 0.5 MPa H_2) by varying the *m*-DNB **1** concentration in ethanol (0.06–0.12 mol dm^{-3}) over the supported 1% Pd/TiO_2 catalysts with Pd NPs 5.0–6.9 nm in size and a dispersion of 16–23%.

This work was supported by Ministry of Science and Higher Education of the Russian Federation (project no. 075-15-2023-585).

Online Supplementary Materials

Supplementary data associated with this article can be found in the online version at doi: 10.1016/j.mencom.2024.06.039.

References

1 J. Wu and C. Darcel, *Adv. Synth. Catal.*, 2023, **365**, 948.

2 P. A. Forero-Cortés and A. M. Haydl, *Org. Process Res. Dev.*, 2019, **23**, 1478.

3 J. Song, Z.-F. Huang, L. Pan, K. Li, X. Zhang, L. Wang and J.-J. Zou, *Appl. Catal., B*, 2018, **227**, 386.

4 K. Murugesan, T. Senthamarai, V. G. Chandrashekhar, K. Natte, P. C. J. Kamer, M. Beller and R. V. Jagadeesh, *Chem. Soc. Rev*., 2020, **49**, 6273.

5 G. Liu, C. Chen and J. Chen, *J. Phys. Chem. C*, 2023, **127**, 4375.

6 Z.-N. Hu, J. Liang, K. Ding, Y. Ai, Q. Liang and H.-B. Sun, *Appl. Catal., A*, 2021, **626**, 118339.

7 Z.-N. Hu, Y.Ai, L. Liu, Y. Chen, X. Song, J. Li, J. Yu, H. Tian, R. Guo, H.-B. Sun, J. Hu and Q. Liang, *ChemistrySelect*, 2019, **4**, 8960.

8 R. M. Mironenko, O. B. Belskaya, L. N. Stepanova, T. I. Gulyaeva, M. V. Trenikhin and V. A. Likholobov, *Catal. Lett.*, 2020, **150**, 888.

9 B. Zeynizadeh, F. M. Aminzadeh and H. Mousavi, *Res. Chem. Intermed*., 2021, **47**, 3289.

10 L. Qin, G. Zeng, C. Lai, D. Huang, C. Zhang, M. Cheng, H. Yi, X. Liu, C. Zhou, W. Xiong, F. Huang and W. Cao, *Sci. Total Environ.*, 2019, **652**, 93.

11 M. Miyazaki, K. Ariyama, S. Furukawa, T. Takayama and T. Komatsu, *ChemistrySelect*, 2021, **6**, 5538.

12 Y. Sheng, X. Lin, S. Yue, Y. Liu, X. Zou, X. Wang and X. Lu, *Adv. Mater.*, 2021, **2**, 6722.

13 E. V. Shuvalova and O. A. Kirichenko, *Mendeleev Commun.*, 2021, **31**, 875.

14 A. L. Nuzhdin, I. A. Shchurova, M. V. Bukhtiyarova, P. E. Plyusnin, N. A. Alekseyeva, S. V. Sysolyatin and G. A. Bukhtiyarova, *Kinet. Catal.*, 2023, **64**, 25 (*Kinet. Katal*., 2023, **64**, 31).

15 A. Das, S. Mondal, K. M. Hansda, M. K. Adak and D. Dhak, *Appl. Catal., A*, 2023, **649**, 118955.

16 A. V. Rassolov, P. V. Markov, G. N. Baeva, D. A. Bokarev, A. R. Kolyadenkov, A. E. Vaulina and A. Yu. Stakheev, *Mendeleev Commun.*, 2023, **33**, 673.
17 L. Wang, E. Guan, J. Zhang, J. Yang, Y. Zhu, Y. Han, M. Yang, C. Cen, G. Fu, B. C. Gates and F.-S. Xiao, *Nat. Commun.*, 2018, **9**, 1362.
18 K. Vikanova and E. Redina, *Russ. J. Phys. Chem.*, 2018, **92**, 2374 (*Zh. Fiz. Khim.*, 2018, **92**, 1846).
19 X. Shi, X. Wang, X. Shang, X. Zou, W. Ding and X. Lu, *ChemCatChem*, 2017, **9**, 3743.
20 P. A. Simonov, A. V. Romanenko and V. A. Likholobov, *Solid Fuel Chem.*, 2014, **48**, 364.
21 R. M. Mironenko, O. B. Belskaya, T. I. Gulyaeva, M. V. Tenikhin and V. A. Likholobov, *Catal. Commun*., 2018, **114**, 46.
22 O. B. Belskaya, R. M. Mironenko, V. P. Talsi, V. A. Rodionov, S. V. Sysolyatin and V. A. Likholobov, *Procedia Eng.*, 2016, **152**, 110.
23 O. B. Belskaya, R. M. Mironenko, V. P. Talsi, V. A. Rodionov, T. I. Gulyaeva, S. V. Sysolyatin and V. A. Likholobov, *Catal. Today*, 2018, **301**, 258.
24 I. A. Shchurova, N. A. Alekseyeva, S. V. Sysolyatin and V. V. Malykhin, *Molecules*, 2022, **27**, 8595.
25 P. Ji, X. Han, Z. Li, Q. Zhang, W. Cheng, J. Sheng, R. Fan, Q. Liao, C. Zhang and H. Li, *Appl. Surface Sci.*, 2023, **636**, 157782.
26 X. Duan, J. Yin, M. Huang, A. Feng, W. Fu, H. Chen, Z. Huang, Y. Ding and J. Zhang, *Chem. Eng. Sci*., 2022, **248**, 117113.
27 J. J. Martínez, E. X. Aguilera, J. Cubillos, H. Rojas, A. Gómez-Cortés and G. Díaz, *J. Mol. Catal. A: Chem.*, 2019, **465**, 54.
28 V. L. Khilnani and S. B. Chandalia, *Org. Process Res. Dev.*, 2001, **5**, 263.
29 Q. Song, W. D. Wang, K. Lu, F. Li, B. Wang, L. Sun, J. Ma, H. Zhu, B. Li and Z. Dong, *Chem. Eng. J*., 2021, **415**, 128856.
30 O. A. Kirichenko, E. A. Redina, G. I. Kapustin, M. S. Chernova, A. A. Shesterkina and L. M. Kustov, *Catalysts*, 2021, **11**, 583.
31 H. Cheng, W. Lin, X. Li, C. Zhang and F. Zhao, *Catalysts*, 2014, **4**, 276.
32 X. Duan, J. Tu, A. R. Teixeira, L. Sang, K. F. Jensen and J. Zhang, *React. Chem. Eng.*, 2020, **5**, 1751.

Received: 9th February 2024; Com. 24/7391